

## Recombinant Adenovirus Induces Maturation of Dendritic Cells via an NF- $\kappa$ B-Dependent Pathway

ADRIAN E. MORELLI,<sup>1,2\*</sup> ADRIANA T. LARREGINA,<sup>3</sup> RAYMOND W. GANSTER,<sup>2</sup>  
ALAN F. ZAHORCHAK,<sup>1,2</sup> JEFFREY M. PLOWEY,<sup>3</sup> TAKUYA TAKAYAMA,<sup>1,2</sup> ALISON J. LOGAR,<sup>1,2</sup>  
PAUL D. ROBBINS,<sup>4</sup> LOUIS D. FALO,<sup>3</sup> AND ANGUS W. THOMSON<sup>1,2,4</sup>

*Thomas E. Starzl Transplantation Institute,<sup>1</sup> Department of Surgery,<sup>2</sup> Department of Molecular Genetics and Biochemistry,<sup>4</sup> and Department of Dermatology and the University of Pittsburgh Cancer Institute,<sup>3</sup> University of Pittsburgh Medical Center, Pittsburgh, Pennsylvania 15213-2582*

Received 5 May 2000/Accepted 12 July 2000

**Recombinant adenovirus (rAd) infection is one of the most effective and frequently employed methods to transduce dendritic cells (DC). Contradictory results have been reported recently concerning the influence of rAd on the differentiation and activation of DC. In this report, we show that, as a result of rAd infection, mouse bone marrow-derived immature DC upregulate expression of major histocompatibility complex class I and II antigens, costimulatory molecules (CD40, CD80, and CD86), and the adhesion molecule CD54 (ICAM-1). rAd-transduced DC exhibited increased allostimulatory capacity and levels of interleukin-6 (IL-6), IL-12p40, IL-15, gamma interferon, and tumor necrosis factor alpha mRNAs, without effects on other immunoregulatory cytokine transcripts such as IL-10 or IL-12p35. These effects were not related to specific transgenic sequences or to rAd genome transcription. The rAd effect correlated with a rapid increase (1 h) in the NF- $\kappa$ B-DNA binding activity detected by electrophoretic mobility shift assays. rAd-induced DC maturation was blocked by the proteasome inhibitor *N* $\alpha$ -*p*-tosyl-L-lysine chloromethyl ketone (TLCK) or by infection with rAd-I $\kappa$ B, an rAd-encoding the dominant-negative form of I $\kappa$ B. In vivo studies showed that after intravenous administration, rAds were rapidly entrapped in the spleen by marginal zone DC that mobilized to T-cell areas, a phenomenon suggesting that rAd also induced DC differentiation in vivo. These findings may explain the immunogenicity of rAd and the difficulties in inducing long-term antigen-specific T-cell hyporesponsiveness with rAd-transduced DC.**

As professional antigen-presenting cells (APC), dendritic cells (DC) exhibit the unique ability to stimulate both naive and memory T lymphocytes and play a critical role in central and peripheral T-cell tolerance (3, 4, 34, 55, 58). Their potential to determine the balance between immunity and tolerance makes DC targets for the therapeutic manipulation of immune responses against tumor cells or microorganisms or for the control of undesired immune reactions against allo- or autoantigens. In this respect, gene transfer approaches have been explored in an effort to potentiate the adjuvant (12, 29) or tolerogenic properties of DC (30, 35, 57). Recombinant adenovirus (rAd) has been demonstrated to be one of the most effective vehicles to deliver foreign DNA into DC (1, 15, 16, 29, 41, 59, 71). However, a fundamental problem with the use of replication-deficient rAd is that they generate the rapid development of natural killer (NK) cell and cytotoxic T-lymphocyte (CTL) responses that eliminate rAd-infected cells and induce neutralizing antibodies (Abs) that "limit" readministration of the same rAd serotype (65–67). The immunogenicity of rAd is a particular drawback when long-term transgene expression is required or when transduced DC are employed to generate antigen-specific tolerance for therapy of graft rejection or autoimmune diseases (26, 30, 35, 65–67). Although the mechanistic basis of rAd immunogenicity is unknown, evidence has accumulated that this phenomenon is associated with the expression of transgene and viral proteins (17, 26, 53, 67) and the active participation of DC (52). Thus, human DC infected with E1a<sup>−</sup> rAd induce the generation of virus-specific CTLs in vitro

(52). Moreover, DC infected ex vivo with rAd-encoding cDNAs unrelated to immunostimulatory molecules (e.g., reporter genes) exhibit a higher T-cell stimulatory ability compared to non-transduced DC (27, 30, 35).

There is evidence that DC-virus interaction affects DC activity in different ways. Thus, whereas influenza virus infection augments DC stimulatory activity, measles or human immunodeficiency viruses silence the host immune response through negative effects on DC function (6). With respect to rAd, different groups have recently reported contradictory effects on DC (25, 27, 46, 59, 71). Zhong et al. (71) and Tillman et al. (59) concluded that rAd is a nonperturbing vector for DC. By contrast, Rea et al. (46) demonstrated that rAd infection activates human DC.

NF- $\kappa$ B is an evolutionarily conserved family of regulatory, DNA-binding transcription factors that are resident in the cytoplasm in various homo- and heterodimeric associations (2, 28, 38). NF- $\kappa$ B factors play a crucial role during generation and maturation of myeloid DC (9, 10, 19, 43, 45, 48, 64). NF- $\kappa$ B is sequestered in the cytoplasm by the inhibitory  $\kappa$ B proteins, I $\kappa$ B $\alpha$  and I $\kappa$ B $\beta$ . Signal transduction results in the phosphorylation and subsequent ubiquitination of I $\kappa$ B, which serves to target I $\kappa$ B protein for degradation by the proteasome. As a result of I $\kappa$ B proteolysis, the NF- $\kappa$ B dimers are liberated for nuclear translocation, bind to specific DNA sequence elements ( $\kappa$ B motifs), and regulate target gene transcription by interactions with the general transcription machinery. Recent progress has dissected the signaling pathway by which tumor necrosis factor alpha (TNF- $\alpha$ ), interleukin-1 $\beta$  (IL-1 $\beta$ ), and bacterial lipopolysaccharide (LPS) activate the nuclear translocation of NF- $\kappa$ B. After cytokine-receptor engagement, the FADD/MORT/MyD family proteins are recruited to the cytoplasmic tail of the receptor; subsequently,

\* Corresponding author. Mailing address: Department of Surgery, University of Pittsburgh Medical Center, E1504 Biomedical Science Tower, 200 Lothrop St., Pittsburgh, PA 15213. Phone: (412) 624-6627. Fax: (412) 624-1172. E-mail: morelli@imap.pitt.edu.

FADD/MORT/MyD proteins interact with and activate either the TRAF2 or TRAF6 proteins. Activated TRAF binds to and activates the NF- $\kappa$ B inducing kinase complex, which in turn phosphorylates and activates the inhibitory  $\kappa$ B kinase complex. Activated inhibitory kinase complex can directly phosphorylate serines 32 and 36 of I $\kappa$ B, which targets I $\kappa$ B for proteolysis, thereby releasing NF- $\kappa$ B dimers to enter the nucleus (2, 28, 38).

In the present study, we investigated the effects of rAd on mouse DC, both in vitro and in vivo. We show that DC infected with rAd exhibited increased expression of major histocompatibility complex (MHC), adhesion, and costimulatory molecules and enhanced allostimulatory function. After rAd infection, increased levels of IL-6, IL-12p40, IL-15, gamma interferon (IFN- $\gamma$ ), and TNF- $\alpha$  mRNAs were observed, whereas transcription of IL-12p35, IL-10, or transforming growth factor  $\beta$ 1 (TGF- $\beta$ 1) remained unaffected, or even decreased. DC activation after rAd infection was not associated with any particular transgenic sequence and was independent of viral transcription. However, the viral effect on DC correlated with rapid nuclear translocation of NF- $\kappa$ B, which was blocked either by the proteasome inhibitor  $N\alpha$ -p-tosyl-L-lysine chloromethyl ketone (TLCK) or by an rAd encoding the mutant form of I $\kappa$ B $\alpha$ , both inhibitors (by different mechanisms) of NF- $\kappa$ B nuclear translocation. Our in vivo studies reveal that splenic DC in the marginal zone were among the first targets of rAd infection after intravenous (i.v.) administration. In agreement with the in vitro results, rAd induced rapid mobilization of immature DC from the marginal zone into the T-cell-dependent areas, an observation indicative of DC activation in vivo.

#### MATERIALS AND METHODS

**Experimental animals.** Ten- to twelve-week-old C57BL/10 (B10; *H2K<sup>b</sup> I-A<sup>b</sup> I-E<sup>a</sup>*) and C3H/He (C3H; *H2K<sup>k</sup> I-A<sup>k</sup> I-E<sup>k</sup>*) mice were purchased from The Jackson Laboratory (Bar Harbor, Maine). Animals were maintained in the specific-pathogen-free facility of the University of Pittsburgh Medical Center.

**Reagents.** Mouse recombinant granulocyte-macrophage colony-stimulating factor (GM-CSF) was a gift from the Schering-Plough Research Institute (Kenilworth, N.J.), and mouse rIL-4 was purchased from R&D (Minneapolis, Minn.). The NF- $\kappa$ B inhibitor TLCK and 7-amino-actinomycin D (7-ADD) were purchased from Calbiochem (San Diego, Calif.).

**Generation of BM DC.** The method was modified from one described earlier (22,37). Briefly, bone-marrow (BM) cells from femurs and tibias of B10 mice were depleted of red blood cells by lysis with ammonium chloride. NK cells, granulocytes, erythroid precursors, and T and B cells were killed by labeling with a cocktail of monoclonal Abs (MAbs; anti-NK-1.1, anti-Gr-1, anti-TER-119/erythroid cells, anti-CD4, anti-CD8, and anti-CD45R/B220; all MAbs were from PharMingen, San Diego, Calif.), followed by incubation with low-toxicity rabbit complement (Cedarlane) BM cells were cultured in RPMI 1640 (Life Technologies, Grand Island, N.Y.) with 10% heat-inactivated fetal calf serum (Life Technologies), glutamine, nonessential amino acids, sodium pyruvate, HEPES, 2-mercaptoethanol, and penicillin-streptomycin, supplemented with 1,000 U of murine rGM-CSF and 1,000 U of murine rIL-4 per ml. Culture medium was replaced at day 3. At day 5, nonadherent cells were removed, and fresh medium with cytokines was added. Two days later (day 7) approximately 60 to 90% of the new population of nonadherent cells was CD11c<sup>+</sup> BM DC, with a predominance of immature DC (CD11c<sup>+</sup> CD86<sup>-</sup> cells) (Fig. 1A). In experiments in which the whole population of BM cells (day 7) was infected with rAd, flow cytometric analysis was performed exclusively on the CD11c<sup>+</sup> DC subset (CD11c is a DC-restricted marker in the mouse). In other cases, CD11c<sup>+</sup> CD86<sup>-</sup> and CD11c<sup>+</sup> CD86<sup>+</sup> BM DC were isolated by flow sorting (purity, 90 to 94%). For molecular analysis, CD11c<sup>+</sup> BM DC were positively selected by incubating BM cells cultured in GM-CSF plus IL-4 (day 7) with a bead-conjugated hamster anti-mouse CD11c MAb (Miltenyi Biotec, Auburn, Calif.), followed by passage through a paramagnetic column (Miltenyi) (DC purity, 90 to 93%). Because of the variability in the percentage of DC and in the immature/mature DC ratio in each experiment, each had its own nontreated control. Results were compared only within and not between experiments.

**rAd vectors.** E1<sup>-</sup> E3<sup>-</sup> deleted rAds included (i) Add1434 (rAd-Control), encoding no transgene or transpromoter, kindly provided by A. Shaked (Department of Surgery, University of Pennsylvania) (44); (ii) rAd-EGFP, encoding the enhanced variant of the *Aequorea victoria* green fluorescent protein (EGFP) cDNA; (iii) rAd-LacZ, encoding the *Escherichia coli*  $\beta$ -galactosidase cDNA; (iv) rAd-Luc, encoding the luciferase cDNA; and (v) rAd-I $\kappa$ B $\alpha$ , encoding the cDNA

for the mutant form of I $\kappa$ B $\alpha$ , kindly provided by D. A. Brenner (University of North Carolina) (24). All transgenes were under the control of the hCMV-MIEp. rAds were scaled up and purified by a 1,1,2-trichloro-trifluoroethane extraction procedure (Sigma), followed by two CsCl gradients (Life Technologies). CsCl was removed from viral bands by dialysis against 2 liters of buffer (Tris, 10 mM; MgCl<sub>2</sub>, 1 mM; NaCl, 135 mM [pH 7.5]). The final dialysis was performed against the same buffer containing 10% glycerol. Virus stocks were tested for the presence of replication-competent Ad as described elsewhere (18) and preserved at -80°C. Viral titers were measured by standard endpoint dilution assay using 293 cells. All Ad preparations were analyzed for endotoxin (LPS) by using the *Limulus* amoebocyte lysate test (E-TOXATE; Sigma) according to the manufacturer's protocol. The detection limit of the test was 0.015 endotoxin units/10<sup>10</sup> PFU/ml. All experiments were done with viral aliquots that tested negative for endotoxin.

**Flow cytometry.** For triple color labeling, BM DC were blocked with normal goat serum (1:10, 10 min at 4°C) and then incubated (1 h at 4°C) with (i) biotin-conjugated hamster anti-mouse CD11c MAb (HL3), (ii) phycoerythrin (PE)-conjugated rat anti-mouse CD86 MAb (GL1), and (iii) one of the following fluorescein isothiocyanate (FITC)-conjugated MAbs: mouse anti-H2K<sup>b</sup> (AF6-88.5), mouse anti-IA<sup>b</sup>  $\beta$  chain (25-9-17), hamster anti-mouse CD40 (HM40-3), hamster anti-mouse CD80 (16-10A1), rat anti-mouse CD11b (M1/70), or hamster anti-mouse CD54 (3E2). Incubation with primary MAb was followed by treatment with Cy-Chrome-conjugated streptavidin (PharMingen) at 1:2,000 for 30 min at 4°C. After staining, cells were washed and fixed in 2% paraformaldehyde. For double immunostaining of rAd-infected BM DC, cells were blocked with normal goat serum as described above and then incubated (1 h at 4°C) with (i) PE anti-mouse CD11c MAb and (ii) one of the following FITC-conjugated MAbs: anti-H2K<sup>b</sup>, anti-IA<sup>b</sup>  $\beta$  chain, anti-mouse CD40, anti-mouse CD80, anti-mouse CD86, anti-mouse CD11b, or anti-mouse CD54. After staining, cells were washed and incubated with 7-ADD to exclude dead cells. Appropriate fluorochrome-conjugated species- and isotype-matched, irrelevant MAbs were used as negative controls. All MAbs were purchased from PharMingen. Cytometric analysis was performed using an EPICS Elite flow cytometer (Coulter, Hialeah, Fla.).

**RPA.** RNA was isolated using a total RNA Isolation Kit (PharMingen) from  $5 \times 10^6$  CD11c<sup>+</sup> BM DC highly purified by positive selection with bead-anti-CD11c MAb, followed by passage through a paramagnetic column as described above. RNA was dissolved in RNase-free water and stored at -80°C until use. The RNase protection assay (RPA) for cytokine mRNAs was performed using the RiboQuant Multi-Probe RPA System (PharMingen). Two different multiprobe template kits containing cDNAs encoding mouse IL-2, IL-3, IL-4, IL-5, IL-6, IL-9, IL-10, IL-12p35, IL-12p40, IL-13, IL-15, IFN- $\beta$ , IFN- $\gamma$ , TNF- $\alpha$ , TGF- $\beta$ 1, TGF- $\beta$ 2, TGF- $\beta$ 3, macrophage migration inhibition factor, and the house-keeping genes L32 and glyceraldehyde-3-phosphate dehydrogenase (GAPDH) were used as templates for the T7 polymerase-directed synthesis of [ $\gamma$ -<sup>32</sup>P]UTP labeled antisense RNA probes. Hybridization (16 h at 56°C) of 5  $\mu$ g of each target mRNA with the antisense RNA probes sets was followed by RNase and proteinase K treatment, phenol-chloroform extraction, and ammonium acetate precipitation of protected RNA duplexes. In each RPA, the corresponding antisense RNA probe set ( $3 \times 10^3$  cpm) was included as the molecular weight standard and to examine probe set integrity. Mouse RNA (PharMingen) (positive control) and RNA degradation controls were included. Yeast tRNA served as negative control. Samples were electrophoresed on acrylamide-urea sequencing gels. Dried gels were exposed on Fujifilm X-ray film, with two intensifying screens, at -80°C. Quantification of the bands was performed by densitometry (Personal Densitometers 1; Molecular Dynamics, Sunnyvale, Calif.), followed by assessment using ImageQuantNT software (Molecular Dynamics). The signals from specific mRNAs were normalized to signals from housekeeping genes (L32 and GAPDH) run on each lane to adjust for loading differences.

**Cytokine quantitation.** Enzyme-linked immunosorbent assay (ELISA) kits (OptEIA; PharMingen) were used to quantify murine IL-12 p40/70 and IFN- $\gamma$  in 48-h supernatants of rAd-transduced DC. The detection limits for IL-12 and IFN- $\gamma$  were 6.25 and 15.6 pg/ml, respectively.

**Allostimulatory activity (MLR).** B10 BM DC (day 7) were purified by sorting into CD11c<sup>+</sup> CD86<sup>-</sup> (immature) DC and CD11c<sup>+</sup> CD86<sup>+</sup> (mature) DC. Both subpopulations were employed as stimulators in 72-h primary mixed leukocyte reactions (MLR) using nylon wool column purified naive allogeneic (C3H) splenic T cells as responders (30,35). In experiments with rAd-infected DC, CD11c<sup>+</sup> BM DC infected with increasing doses of virus and purified by positive selection with paramagnetic columns were employed as stimulators. As controls, nontransduced B10 BM DC, or B10 splenocytes, or C3H splenocytes were used as stimulators.

**Preparation of nuclear protein fractions and electrophoretic mobility shift assays (EMSAs).** BM DC (day 7) were purified by labeling with bead anti-CD11c MAb, followed by passage through paramagnetic columns, and infected with rAd-Control or rAd-I $\kappa$ B (multiplicity of infection [MOI] of 100) for 1, 3, or 18 h. To prepare nuclear extracts, BM DC were pelleted, resuspended in 0.5 ml of buffer A (10 mM HEPES [pH 7.9], 1.5 mM MgCl<sub>2</sub>, 10 mM KCl, and 0.5% Nonidet P-40 [NP-40]) and disrupted by gently pipetting. Nuclei were washed in buffer B (buffer A without NP-40), and nuclear proteins were extracted with 20 mM HEPES (pH 7.9), 10% glycerol, 1.5 mM MgCl<sub>2</sub>, 420 mM KCl, and 0.2 mM EDTA. All steps were performed on ice or at 4°C. All buffers contained 1 to 2

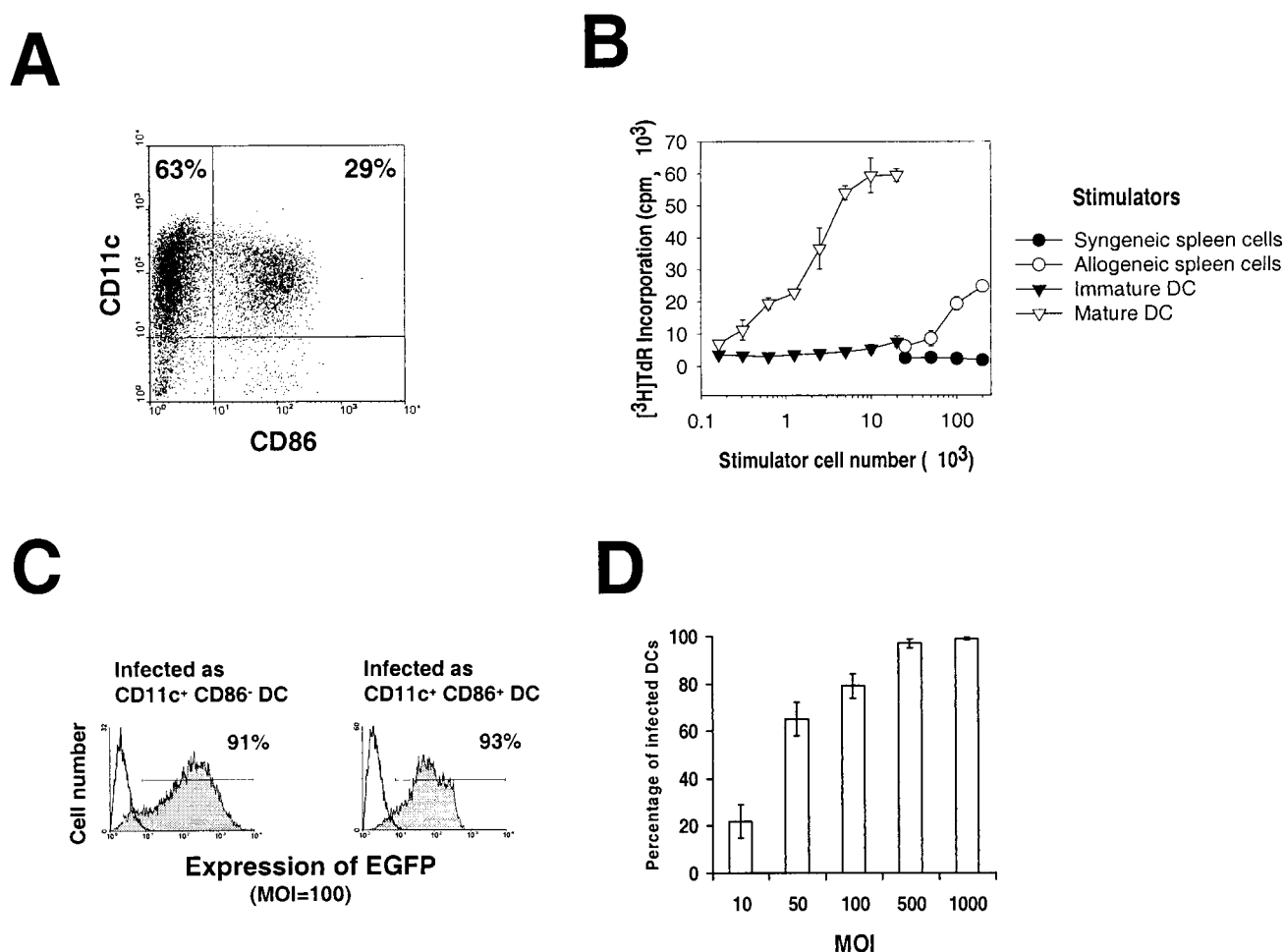


FIG. 1. (A) BM DC generated in GM-CSF plus IL-4 (day 7) as described in Materials and Methods, labeled, and analyzed by flow cytometry. Two populations of DC were detected: CD11c<sup>+</sup> CD86<sup>-</sup> immature DC (upper left quadrant) and CD11c<sup>+</sup> CD86<sup>+</sup> DC (upper right quadrant). (B) Allostimulatory activity of gamma-irradiated, purified immature CD11c<sup>+</sup> CD86<sup>-</sup> (▼) or mature CD11c<sup>+</sup> CD86<sup>+</sup> B10 DC (▽), assessed using naive C3H (*H2<sup>k</sup>*) splenic T cells as responders in a 3-day MLR. BM DC were propagated as described in Materials and Methods, harvested at day 7, purified by flow sorting, and set up at various concentrations with  $2 \times 10^5$  responder T cells. [<sup>3</sup>H]thymidine (TdR) was added 18 h before harvesting. The MLR stimulatory activity of freshly-isolated B10 (○) or C3H (●) bulk spleen cells is also shown. The results are expressed as mean counts per minute  $\pm$  1 SD, and are representative of at least three separate experiments. (C) Transduction efficiency of immature (CD11c<sup>+</sup> CD86<sup>-</sup>) and mature (CD11c<sup>+</sup> CD86<sup>+</sup>) DC purified by sorting and infected with rAd-EGFP (at an MOI of 100). Transgene expression was evaluated 24 h later by flow cytometry. (D) Transduction efficiency of DC infected for 2 days with increasing MOIs of rAds and detected by flow cytometry. In panels C and D the transgene expression was evaluated exclusively on CD11c<sup>+</sup> cells. Dead cells were excluded by 7-ADD staining. No positive cells were detected in noninfected controls or in cells infected with rAd-Control (data not shown). The data are representative of three independent experiments.

$\mu$ g each of aprotinin, benzamidin, chymostatin, leupeptin, and pepstatin per ml; 0.2 mM phenylmethylsulfonyl fluoride, 0.5 mM dithiothreitol, and 0.1  $\mu$ M sodium vanadate. Protein concentrations were measured by using the Bio-Rad protein assay with bovine serum albumin as a standard. The NF- $\kappa$ B binding sequence from the immunoglobulin  $\kappa$  light chain enhancer (5' AGT TGA GGG GAC TTT CCC AGG C 3') was used as a probe. DNA probes were end labeled with [<sup>32</sup>P]ATP using T4 polynucleotide kinase (Boehringer Mannheim) and purified on Sephadex G-50 columns (Sigma) equilibrated with TEN (10 mM Tris, 1 mM EDTA, 100 mM NaCl) as described by the manufacturer (Sigma). A portion (5  $\mu$ l [1  $\mu$ g]) of each sample of nuclear protein was incubated with  $\sim 10^5$  cpm of <sup>32</sup>P-labeled consensus NF- $\kappa$ B oligonucleotide (0.5 ng) for 45 min at room temperature. The nuclear proteins and NF- $\kappa$ B probe were incubated in buffer (10 mM Tris, pH 7.5; 10% glycerol; 0.2% NP-40). Poly(dI-dC) (Boehringer Mannheim) was included as nonspecific competitor DNA. Protein-DNA complexes were resolved on 4% nondenaturing polyacrylamide gels in running buffer (450 mM Tris borate, 1  $\mu$ M EDTA; pH 8.0). After electrophoresis, gels were dried and subjected to autoradiography. Antibody supershift experiments included the addition of 1  $\mu$ l of anti-p50 or anti-p65 polyclonal antibodies (Santa Cruz Biotechnology, Santa Cruz, Calif.).

**Immunofluorescence staining of tissue sections.** Spleen samples were embedded in Tissue-Tek OCT (Miles Laboratories, Inc., Elkhart, Ind.), snap frozen in isopentane-liquid nitrogen, and stored at  $-80^\circ\text{C}$  until further use. To preserve the tissue localization of EGFP, spleens from animals injected with rAd-EGFP were fixed in 2% paraformaldehyde (2 h at  $4^\circ\text{C}$ ) and cryopreserved in 30%

sucrose-phosphate-buffered saline (PBS) overnight, and snap frozen. Cryostat sections (8  $\mu$ m) were air dried, fixed in acetone (10 min at  $4^\circ\text{C}$ ), blocked with normal goat serum, and incubated with PE-labeled anti-mouse CD11c MAb and FITC-labeled anti-mouse CD3 $\epsilon$  MAb (145-2C11; PharMingen), for 1 h at room temperature. Sections were fixed in 2% paraformaldehyde and mounted with glycerol-PBS (pH 7.0). Slides were examined with a Zeiss Axiovert 135 microscope equipped with appropriate filters. Fluorescence was visualized using a cooled charge-coupled-device camera (Photometrics CH250; Photometrics, Tucson, Ariz.). Signals from different fluorochromes were acquired independently, and final montages were edited using the Adobe Photoshop software program (Adobe Systems, Mountain View, Calif.).

**Statistical analysis.** Results are expressed as means  $\pm$  one standard deviation (SD). Comparisons between different means were performed by analysis of variance, followed by the Student Newman-Keuls test. Comparison between two means was performed by the Student *t* test. A *P* value of  $<0.05$  was considered significant.

## RESULTS

**Immature and mature BM DC are infected by rAd.** BM DC generated in vitro with GM-CSF plus IL-4 showed at day 7 a mixed population of CD11c<sup>+</sup> CD86<sup>-</sup> ( $69 \pm 11\%$ ) and CD11c<sup>+</sup>

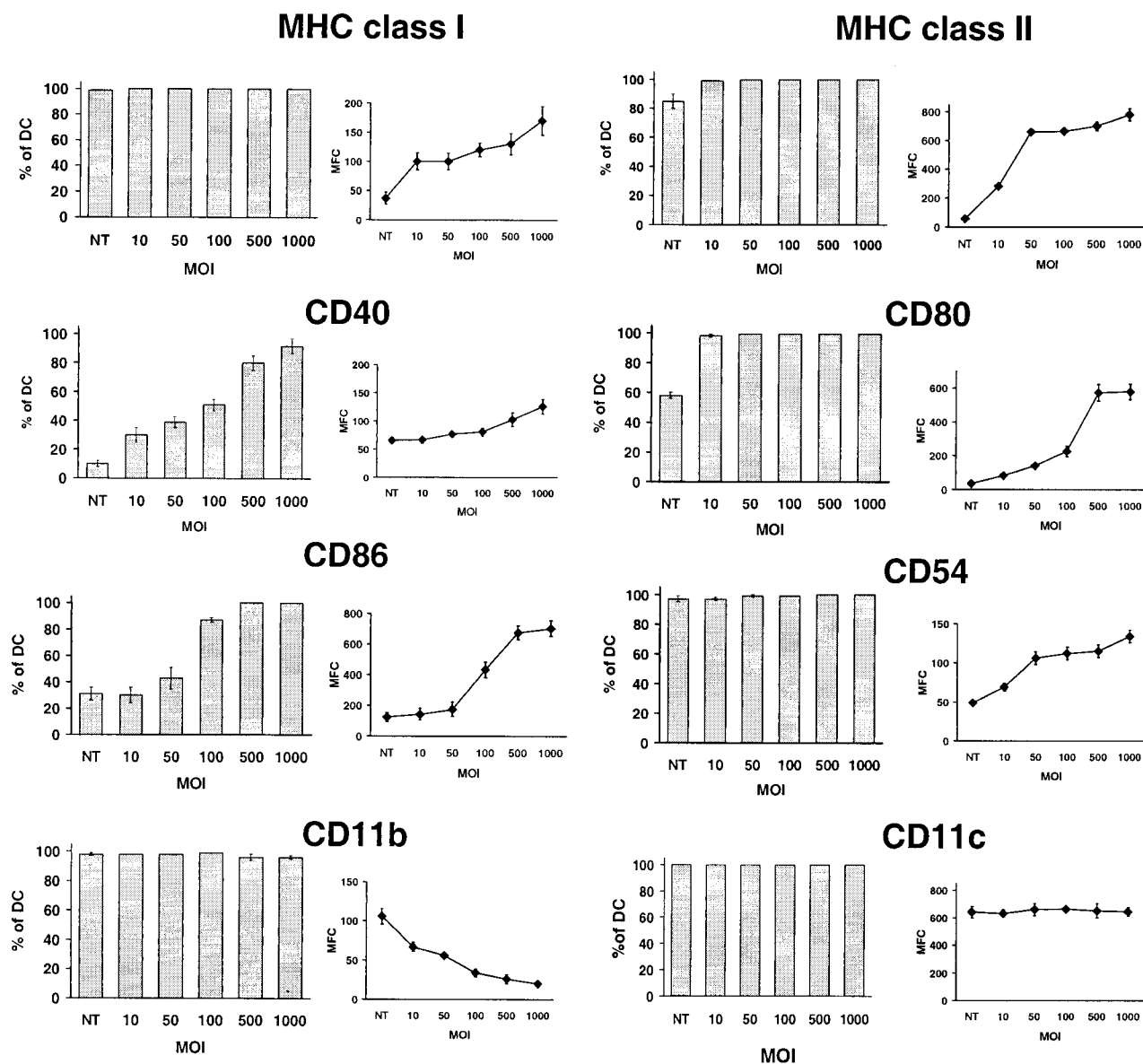


FIG. 2. Infection of BM DC with rAd modifies the expression of cell surface markers. DC transduced with increasing MOIs of rAd-Control were maintained in GM-CSF plus IL-4 for 48 h and then labeled and analyzed by flow cytometry. Cells were labeled with a PE-conjugated anti-CD11c MAb, followed by anti-MHC-I, anti-MHC-II, anti-CD40, anti-CD80, anti-CD86, anti-CD54, and anti-CD11b MAbs, all FITC conjugated. The DC population illustrated was gated according to forward versus side scatter, and positivity for CD11c. Dead cells were excluded by 7-ADD staining. The percentage of CD11c<sup>+</sup> DC positive for each marker (bar diagrams) and the MFC (curves) is detailed. Nontransduced DC (NT) cultured under similar circumstances were included as controls. Results correspond to the mean  $\pm$  the SD of three separate experiments.

CD86<sup>+</sup> (30  $\pm$  8%) DC (Fig. 1A). Triple labeling of the CD11c<sup>+</sup> CD86<sup>+</sup> cells, followed by flow cytometric analysis, revealed surface markers of immature myeloid DC (MHC class I<sup>lo</sup> [MHC-I<sup>lo</sup>], MHC-II<sup>lo</sup>, CD40<sup>lo</sup>, CD80<sup>lo</sup>, CD11b<sup>hi</sup>, and CD54<sup>lo</sup>). These cells induced only minimal levels of allogeneic T-cell proliferation in vitro (Fig. 1B). In contrast, CD11c<sup>+</sup> CD86<sup>+</sup> cells exhibited the phenotype of mature DC (MHC-I<sup>hi</sup>, MHC-II<sup>hi</sup>, CD40<sup>+</sup>, CD80<sup>hi</sup>, CD11b<sup>lo</sup>, and CD54<sup>hi</sup>) and triggered a potent allogeneic T-cell response (Fig. 1B).

To test whether there was a difference in the ability of rAd to infect DC at different stages of maturation, BM DC (day 7) were labeled with CyChrome-anti-CD11c and PE-anti-CD86 MAbs, sorted into CD11c<sup>+</sup> CD86<sup>+</sup> and CD11c<sup>+</sup> CD86<sup>+</sup> DC, and infected with rAd-EGFP (MOI = 100). At 24 h after

infection, the expression of EGFP was analyzed by flow cytometry. Figure 1C shows that similar percentages of CD86<sup>+</sup> and CD86<sup>+</sup> BM DC were infected by rAd-EGFP.

The efficiency of rAd-mediated gene delivery to BM DC (day 7) was evaluated after 24 h of infection with rAd-EGFP. Figure 1D illustrates the expression of EGFP detected by flow cytometry on live (7-ADD<sup>+</sup>) CD11c<sup>+</sup> DC. Maximum infectivity was achieved at an MOI of 500. No positivity was found in noninfected cells or in cells infected with rAd-Control (data not shown). The mortality of rAd-transduced BM DC (evaluated by 7-ADD labeling and flow cytometry) did not increase significantly ( $P > 0.05$ ) 24 to 48 h after infection, when MOIs of from 10 to 500 were used (not shown).

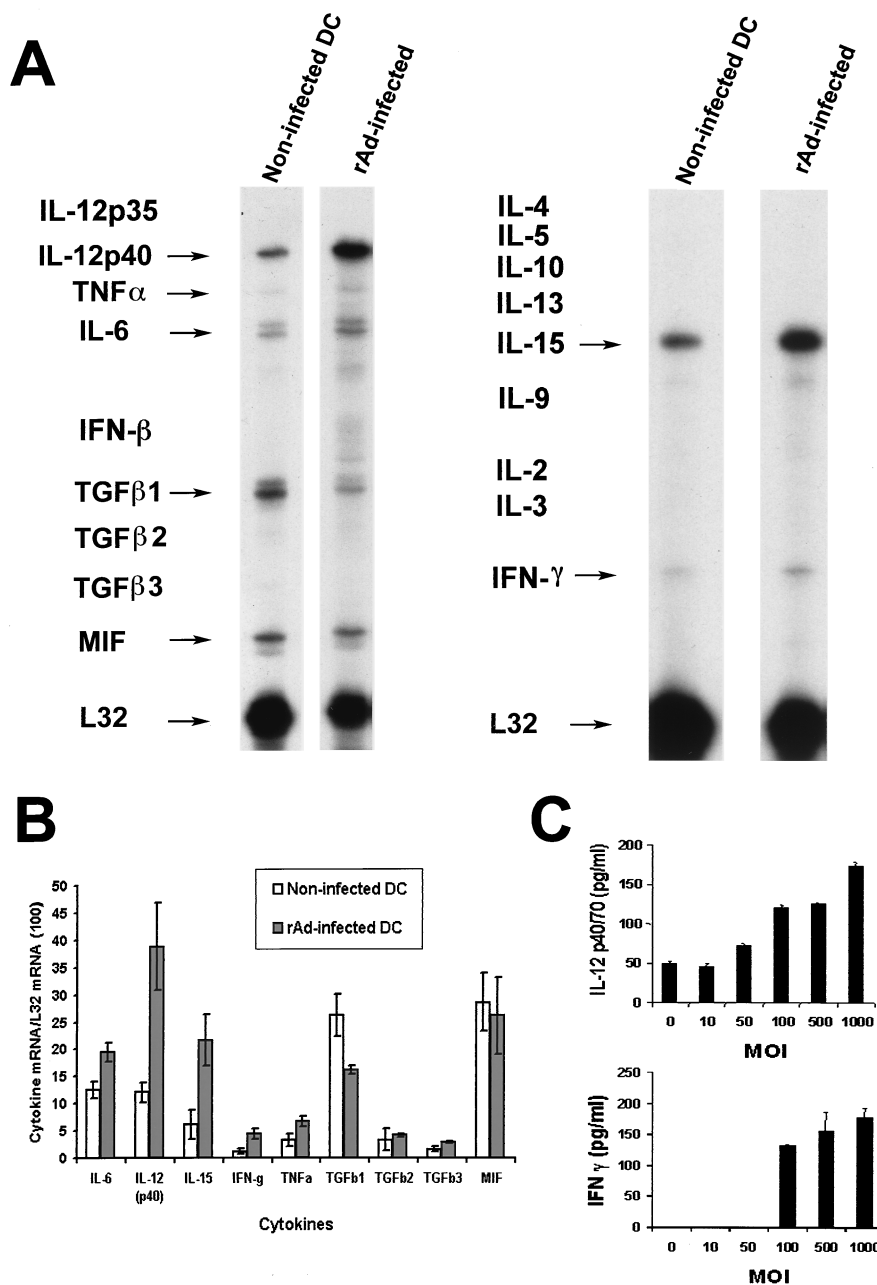


FIG. 3. (A) Comparison of cytokine mRNA expression in noninfected CD11c<sup>+</sup> BM DC or in DC transduced with an MOI of 100 of rAd-Control. mRNA was isolated from DC purified with bead anti-CD11c staining, followed by passage through a paramagnetic column (Miltenyi). Data are from a single experiment representative of three separate experiments. (B) Quantitative analysis of mRNA cytokine gene expression. Densitometry analysis of each lane was performed on scanned autoradiographs, and all values are expressed relative to corresponding housekeeping gene transcripts (L32). Densitometric values were pooled from three separate experiments. (C) Production of IL-12 and IFN- $\gamma$  by rAd-transduced DC. IL-12 p40/70 and IFN- $\gamma$  secreted by BM DC cultures (day 7) infected by rAd-Control were quantified by ELISA in 48-h supernatants. Data are representative of two separate experiments.

**rAd increases the expression of MHC antigen, costimulatory molecules, ICAM-1 (CD54), and levels of cytokine mRNAs in BM DC.** The effect of rAd on the cell surface phenotype of BM DC (day 7) was studied 48 h (day 9) after infection with rAd-Control. Nonadherent cells were double labeled, and the specific markers were analyzed by flow cytometry exclusively in live DC (gate: CD11c<sup>+</sup>, 7-ADD<sup>-</sup>). Infection with rAd caused an increase in the intensity of expression (as measured by the mean fluorescence channel [MFC]) and in the percentage DC positive for MHC-II, CD40, CD80, and CD86 (Fig. 2). For

those markers such as MHC-I and CD54 (ICAM-1) that were present on all CD11c<sup>+</sup> BM DC, there was increased intensity of expression (MFC) (Fig. 2). Most changes in the DC phenotype were detected at MOIs of 10 to 100. Consistent with an rAd-associated DC activation-differentiation process, expression of CD11b (an integrin downregulated upon myeloid DC maturation [49]) decreased after rAd infection (Fig. 2). As a control, the intensity of expression of CD11c, a molecule expressed at the same level by immature and mature DC (Fig. 1A), remained stable (Fig. 2).

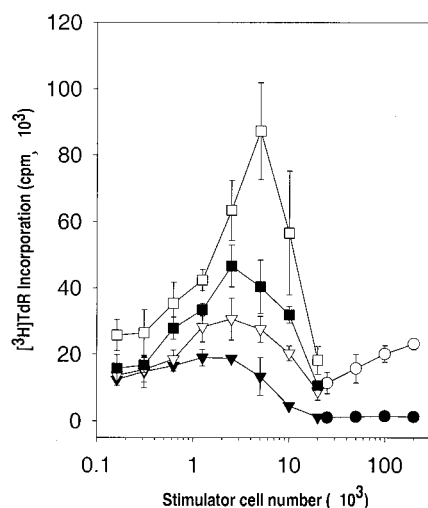


FIG. 4. Allostimulatory activity of gamma-irradiated, noninfected CD11c<sup>+</sup> B10 (*H-2<sup>b</sup>*) BM DC (▼) or CD11c<sup>+</sup> B10 BM DC infected with increasing MOIs of rAd-Control (▽, 50; □, 100; ○, 500), assessed at various concentrations with  $2 \times 10^5$  responder splenic naive C3H (*H-2<sup>k</sup>*) T cells in 3-day MLR experiments. BM DC (day 7) were propagated as described in Materials and Methods, treated with rAd for 24 h, and purified by labeling with bead anti-CD11c MAb and passage through a paramagnetic column. [<sup>3</sup>H]TdR was added 18 h before harvesting. The MLR stimulatory activity of freshly isolated allogeneic (B10 [○]) or syngeneic (C3H [●]) bulk spleen cells is also shown. At very low DC/T-cell ratios ( $<0.625 \times 10^3$  DC/ $2 \times 10^5$  T cells), noninfected DC, rAd (MOI = 50) DC, and rAd (MOI = 100) DC showed similar allostimulatory T-cell activities. At higher DC/T-cell ratios, rAd-infected DC showed increased ability to stimulate allogeneic T cells compared to noninfected DC. The results are expressed as mean counts per minute  $\pm 1$  SD and are representative of three separate experiments.

Activation of cytokine gene expression in relation to rAd infection of BM DC (day 7) was analyzed by RPA 24 h after infection with rAd-Control or with rAd-EGFP (MOI = 100). mRNA was extracted from the CD11c<sup>+</sup> cells isolated by incubation with bead-conjugated anti-CD11c MAb, followed by positive selection with paramagnetic columns. The comparative analysis of cytokine mRNAs in noninfected and rAd-Control-infected BM DC and the quantification of the bands by densitometry are illustrated in Fig. 3A and B. Infection of BM DC with rAd-Control increased the levels of mRNAs for IL-6, IL-12p40, IL-15, IFN- $\gamma$ , and TNF- $\alpha$  and decreased the expression of TGF- $\beta$ 1 mRNA. The increase in IL-12p40 and IFN- $\gamma$  mRNAs was correlated with the levels of protein detected by ELISA in the supernatants 48 h after infection (Fig. 3C) and by intracellular staining of CD11c<sup>+</sup> BM DC by flow cytometry (data not shown). No changes were detected in the level of IL-12 p35 mRNA (detected as an extremely weak band in some of the samples; data not shown) or in the low levels of TGF- $\beta$ 2 and - $\beta$ 3 mRNAs. It was not possible to detect IL-2, IL-3, IL-4, IL-5, IL-9, IL-10, IL-13, or IFN- $\beta$  transcripts in any of the noninfected or rAd-Control transduced samples. Similar data were obtained after CD11c<sup>+</sup> BM DC infection with rAd-EGFP (not shown).

**Infection with rAd increases the allogeneic stimulatory capacity of DC.** The allostimulatory activity of DC following rAd infection was tested in BM DC cultures (day 7) transduced with increasing MOIs of rAd-Control. After 24 h, CD11c<sup>+</sup> BM DC were isolated by positive selection with paramagnetic columns, irradiated, and used as stimulators of allogeneic (C3H) naive T cells in 72-h MLR. CD11c<sup>+</sup> BM DC infected with increasing MOIs of rAd-Control showed an increased capacity to stimulate allogeneic splenic T cells, a phenomenon consistent with the phenotypic changes observed after rAd infection.

The relatively low allostimulatory capacity of noninfected BM DC shown in Fig. 4 was due to the high proportion of immature DC (85%) in the sample.

**Effect of transgene sequences and rAd transcription on BM DC activation.** To investigate whether the changes observed in BM DC were associated with transgenic DNA sequences carried by the virus, we studied (by flow cytometry) the expression of MHC-II and CD86 in the live DC (gate: CD11c<sup>+</sup>, 7-ADD<sup>-</sup>) after infection with rAds with distinct transgenes (rAd-LacZ or rAd-Luc) or without transgene (rAd-Control). The fact that, by 48 h after transduction, the three rAds had upregulated MHC-II and CD86 in CD11c<sup>+</sup> DC (Fig. 5A) suggested that the viral effect might be caused by the nontransgenic rAd genome and/or by viral proteins.

Psoralen UV-inactivated rAd-EGFP (13) was used to analyze whether viral gene transcription was associated with DC activation. The minimum irradiation dose required to inhibit rAd transcription was titrated using rAd-EGFP exposed to UV irradiation for different times and subsequently employed to transduce DC at a high MOI (MOI = 1,000). EGFP expression in CD11c<sup>+</sup> DC was reduced from 100% to <1% after 10 min of irradiation (Fig. 5B). After 48 h of infection with UV-inactivated rAd-EGFP or UV-inactivated rAd-Control (MOI = 100), CD11c<sup>+</sup> DC (gate: CD11c<sup>+</sup>, 7-ADD<sup>-</sup>) upregulated CD86 and MHC-II (Fig. 5C) to the same extent as DC transduced with non-UV-irradiated rAd at the same MOI. Therefore, these results suggest that rAd transcription is not associated with DC activation.

**DC maturation induced by rAd is associated with NF- $\kappa$ B activation.** Because many of the surface molecules and cytokines whose expression was increased by rAd-transduced DC have been shown to be upregulated by NF- $\kappa$ B, we sought to investigate the involvement of NF- $\kappa$ B in rAd-induced DC maturation, using both pharmacologic and genetic inhibition strategies. The peptide TLCK is an inhibitor of proteasome-mediated degradation of the I $\kappa$ B protein and has been shown to inhibit the expression of NF- $\kappa$ B-dependent gene expression (20). We observed a dose-dependent inhibition of the expression of CD86 and MHC-II induced by rAd-Control at an MOI of 100 on DC (gate: CD11c<sup>+</sup>, 7-ADD<sup>-</sup>) (Fig. 6A). Maximal inhibition by TLCK was observed at a concentration of 100 mM. These data are consistent with a role for NF- $\kappa$ B in rAd-induced DC maturation. Since TLCK is a nonspecific inhibitor of trypsin-like proteases, we sought to directly address the role of NF- $\kappa$ B in rAd-induced DC maturation by utilizing rAd engineered to express a mutant I $\kappa$ B protein that replaces serines 32 and 36 with alanine. The mutant I $\kappa$ B protein is not phosphorylated or degraded in response to cytokines and, when overexpressed, functions as a dominant-negative inhibitor of NF- $\kappa$ B-dependent gene transcription (24). Expression of CD86 and MHC-II was analyzed by flow cytometry 24 h after rAd-I $\kappa$ B infection. Inclusion of the mutant I $\kappa$ B transgene prevented the increase in CD86 and MHC-II expression induced by rAd in BM DC (Fig. 6B). These data clearly demonstrate an important role for NF- $\kappa$ B in the upregulation of CD86 and MHC-II in DC after rAd infection.

**rAd increase the nuclear DNA binding activity of NF- $\kappa$ B in BM DC.** Since expression of the mutant I $\kappa$ B transgene prevented the upregulation of CD86 and MHC-II in DC after rAd infection, we sought to address directly the possibility that rAd transduction could activate nuclear NF- $\kappa$ B DNA binding activity in DC by employing the EMSA. Figure 7 shows EMSA results using nuclear protein extracts from purified CD11c<sup>+</sup> DC at various times after rAd infection. Notice that there was an increase in the nuclear NF- $\kappa$ B-DNA binding complex as early as 1 h postinfection, suggesting that rAd is a direct acti-

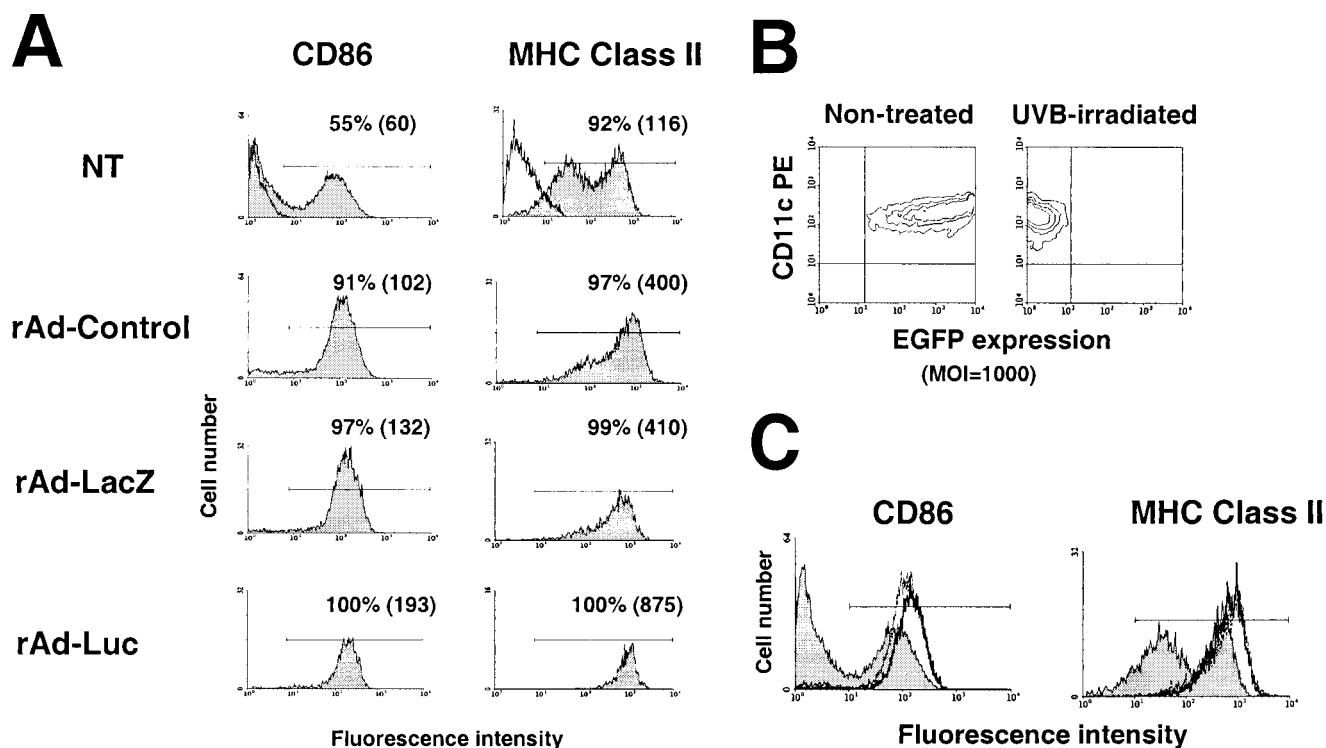


FIG. 5. (A) rAd-induced maturation of DC is not associated with viral transgenic DNA sequences. BM DC cultures (day 7) were infected with three different rAds (MOI = 100). At 48 h after infection, cells were labeled with PE-anti-CD11c MAb in combination with either FITC-anti-CD86 or FITC-anti-MHC-II MABs. Dead cells were excluded by 7-ADD staining. Nontransduced (NT) BM DC cultured under similar circumstances were included as controls. Flow profiles illustrate the expression of CD86 or MHC-II either by nontransduced (NT) CD11c<sup>+</sup> DC or DC infected with a rAd without transgene (rAd-Control) or with two different transgenes (rAd-LacZ and rAd-Luc). The irrelevant isotype controls are the open profiles under NT cells. The percentage of positive cells and the MFC (in parentheses) are detailed. (B and C) Viral transcription is not responsible for DC maturation after rAd infection. (B) EGFP expression by flow cytometric analysis in BM DC infected either with nonirradiated or 10-min UV-treated rAd-EGFP. (C) CD86 and MHC-II expression of CD11c<sup>+</sup> BM DC infected either with UV-irradiated or with nonirradiated rAd-Control (MOI = 100). After 48 h, cells were double labeled for CD11c and either CD86 or MHC-II and then analyzed by flow cytometry. The profiles illustrate expression of CD86 and MHC-II exclusively in the CD11c<sup>+</sup> 7-ADD<sup>-</sup> cells. DC infected either with UV-treated rAd (thick line) or with nonirradiated rAd (thin line) upregulated expression of CD86 and MHC-II compared to noninfected cells (gray profiles) maintained under similar conditions. The data are representative of two separate experiments.

vator of NF- $\kappa$ B signal transduction. A more pronounced increase in NF- $\kappa$ B DNA binding activity was observed at 3 and 18 h postinfection. Importantly, the increase in NF- $\kappa$ B DNA binding activity observed at 3 and 18 h postinfection was blocked if the rAd encoded the dominant-negative I $\kappa$ B mutant transgene. Antibody supershift EMSAs indicated that the p50 NF- $\kappa$ B and, to a lesser extent, the p65 NF- $\kappa$ B protein were the predominant NF- $\kappa$ B proteins activated by rAd infection in DC. Antibodies to the p300/CBP protein were included as a negative control and did not affect the NF- $\kappa$ B DNA complex as expected. These data demonstrate that rAd increased nuclear p50 and p65 NF- $\kappa$ B DNA binding as early as 1 h postinfection, which suggests that rAd is a direct activator of NF- $\kappa$ B in this system. Furthermore, expression of the dominant-negative mutant I $\kappa$ B protein interfered with the rAd-induced nuclear NF- $\kappa$ B DNA binding activity at 3 and 18 h postinfection, while preventing the rAd-induced expression of CD86 and MHC-II (Fig. 6B). These data provide strong evidence for the involvement of NF- $\kappa$ B in the regulation of CD86 and MHC-II gene expression during the maturation of DC induced by rAd.

**i.v. injection of rAd preferentially infects splenic marginal zone DC and induces mobilization of DC into T-cell areas.** DC in the marginal zone of spleen resemble immature DC, whereas interdigitating DC in the T-cell area (periarteriolar lymphoid sheath [PALS]) are mature APC (23, 56, 63). It has been demonstrated in the mouse that i.v. administration of

either LPS or *Toxoplasma gondii* antigen activates marginal DC and elicits their mobilization into the PALS (14, 47). We used this in vivo model to test whether rAd could trigger the maturation and trafficking of marginal zone splenic DC. rAd-EGFP was administered via the tail vein ( $1.5 \times 10^9$  PFU/mouse), and the distribution of DC was analyzed in spleen sections 6, 24, and 48 h after virus injection. As soon as 6 h after rAd administration, EGFP expression was detected exclusively in the marginal zone (Fig. 8A to C). Staining with a PE-anti-CD11c MAb confirmed that marginal zone DC were targets of rAd infection (Fig. 8C). CD11c<sup>+</sup> EGFP<sup>+</sup> cells were also detected. At 24 and 48 h following rAd-EGFP administration, CD11c<sup>+</sup> EGFP<sup>+</sup> DC were detected in the PALS (Fig. 8D), an observation suggesting that rAd initially infected marginal zone DC that later migrated to the PALS. However, this approach allowed us to trace only the movement of those DC that expressed detectable levels of intact EGFP and that may have corresponded to a subset of the entire population of DC influenced by the viral effect. To analyze the mobilization of the entire splenic DC population into T-cell areas, animals were injected i.v. with rAd without reporter gene (rAd-Control/ $1.5 \times 10^9$  PFU/mouse), and tissue sections from different time points were double labeled with PE anti-CD11c MAb for DC and FITC anti-CD3 MAb for T cells. After administration of PBS or in noninjected animals, CD11c<sup>+</sup> DC were clearly distributed in the marginal zone and intermingled with T cells

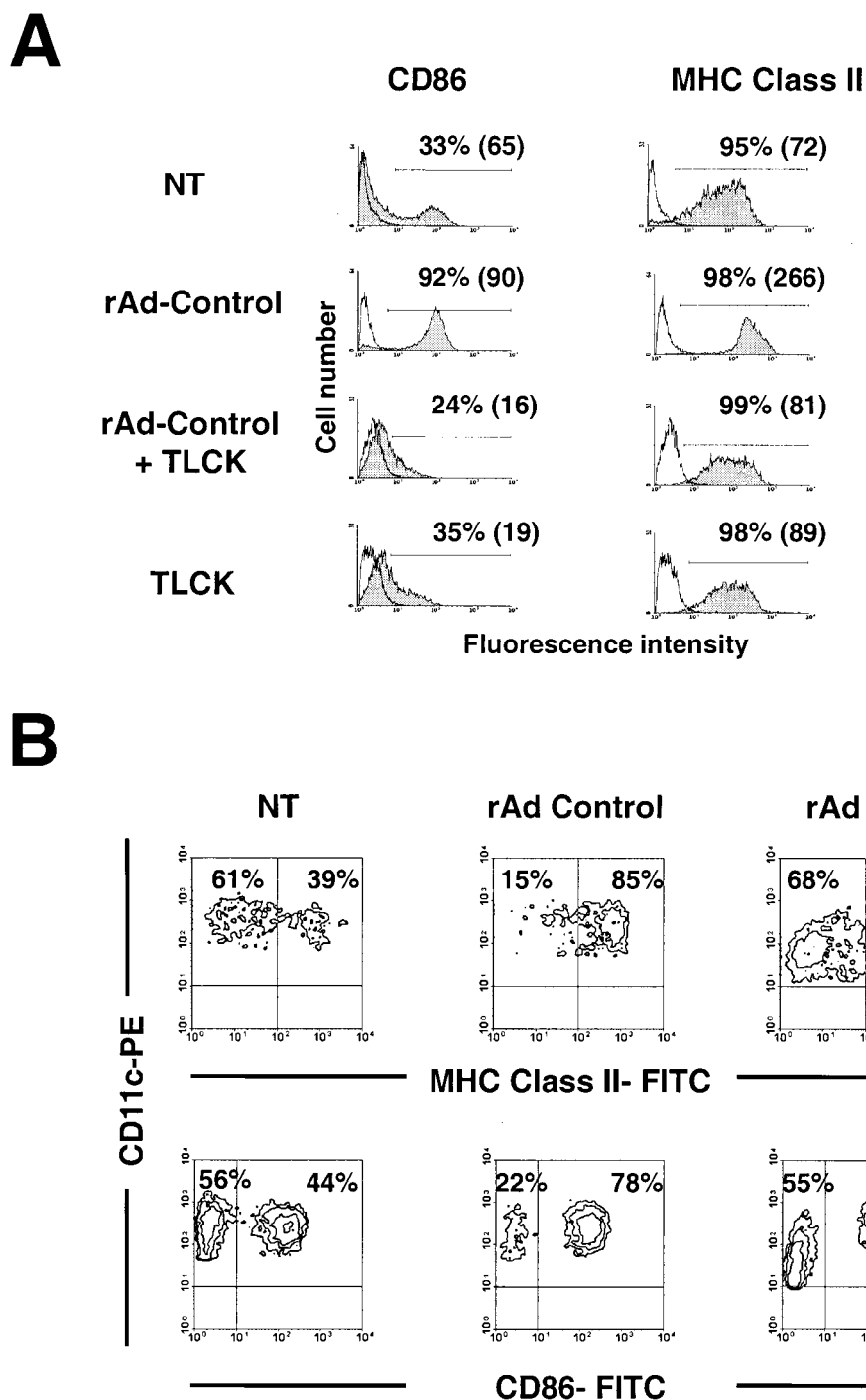


FIG. 6. DC activation associated with rAd infection is blocked by NF- $\kappa$ B inhibitors. (A) BM DC (day 7) were infected with rAd-Control (MOI = 100) and maintained in GM-CSF plus IL-4 with or without the addition of TLCK (TLCK was added 1 h before rAd infection). After 18 h, the expression of CD86 and MHC-II was evaluated exclusively in CD11c<sup>+</sup> 7-ADD cells by double labelling and flow cytometry. The corresponding irrelevant isotype controls are represented by open profiles. Cutoff bars include  $\leq 2$  of negative cells when isotype controls were used. The percentage of positive cells and the MFC (in parentheses) are shown. Nontransduced DC (NT) and NT DC treated with TLCK (TLCK) and cultured under similar conditions were included as controls. (B) Transduction with rAd-I $\kappa$ B $\alpha$  prevented maturation of BM DC induced by rAd infection. Determined 18 h after infection, rAd-I $\kappa$ B $\alpha$  prevented the differentiation of immature DC (CD86<sup>-</sup>, MHC-II<sup>or lo</sup>) into mature DC (CD86<sup>+</sup>, MHC-II<sup>hi</sup>). Data are representative of two separate experiments.

in PALS (Fig. 9A). At 6 and 24 h after virus administration, the number of marginal zone DC decreased, and the population of DC in the PALS increased substantially (Fig. 9B and C). After 48 h, the marginal zones repopulated with CD11c<sup>+</sup> DC (Fig. 9D).

## DISCUSSION

rAd is one of the most effective viral vehicles for delivery of exogenous DNA to a variety of nonreplicating cells, included DC (1, 15, 16, 25, 29, 71). However, the molecular basis of its

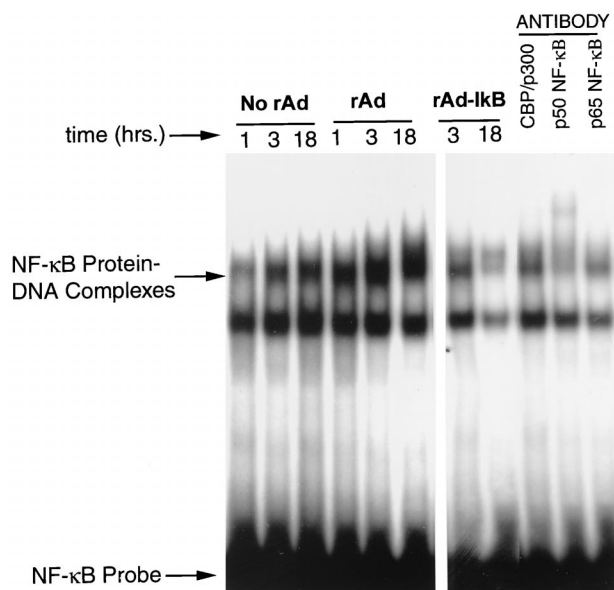


FIG. 7. rAd activates the nuclear binding activity of NF- $\kappa$ B in DC. The gel mobility shift experiment analyzes NF- $\kappa$ B DNA binding activity from nontransduced CD11c<sup>+</sup> purified BM DC or from DC infected with a rAd without transgene (MOI = 100) at different time points postinfection. Highlighted by arrows are the free radiolabeled NF- $\kappa$ B DNA probes and the NF- $\kappa$ B protein-DNA complexes. Notice that rAd increases the NF- $\kappa$ B DNA binding activity as early as 1 h postinfection. The results depicted are representative of four independent experiments. Infection of DC with rAd-I $\kappa$ B encoding the dominant-negative I $\kappa$ B protein inhibited the activation of NF- $\kappa$ B DNA binding activity at 18 h as shown. Addition of antibody to p50 and, to a lesser extent, the p65 NF- $\kappa$ B proteins to the gel shift reactions resulted in an antibody supershift of the NF- $\kappa$ B-DNA complex. Antibody to the nuclear CBP/p300 protein did not interfere with the NF- $\kappa$ B-DNA complex. The data presented are representative of two independent experiments.

strong immunogenicity is not well understood (65–67). Information concerning the effect(s) of rAd on DC, the APC that will determine the outcome of the primary immune response, is still contradictory (25, 27, 29, 46, 59, 71). In this study, we demonstrated that BM DC infected with rAd encoding distinct transgenes upregulated the expression of MHC antigens and costimulatory (CD40, CD80, and CD86) and adhesion (CD54) molecules. As a result, rAd-infected DC became potent stimulators of allogeneic T cells. These rAd effects on DC correlated with the viral input and were even detected at MOIs ranging from 10 to 100, viral doses commonly used for ex vivo DC transduction in gene therapy protocols. Our results agree with those reported recently by Rea et al. (46) using human DC but contrast with those of Zhong et al. (71) and Tillman et al. (59), who concluded that human DC maturation was not a function of rAd infection. As pointed out by Rea et al., in the system used by Zhong et al., immature DC already expressed the maturation marker CD83, a fact that makes it difficult to discriminate between the spontaneous maturation of DC and that induced by rAd (46, 71). The low efficiency of transduction of human DC reported by Tillman et al. after rAd-EGFP infection at an MOI of 100 (<20% compared with ~80% [Fig. 1D] in the present work) may have diluted the effect of the Ad on the DC population (59). Differences in species (mouse versus human DC) may also account for the discrepancies.

We demonstrated that rAd infection increased the transcript levels of IL-6, IL-12p40, IL-15, IFN- $\gamma$ , and TNF- $\alpha$  genes. These data confirm and extend the recent report by Rea et al. (46), in which they showed that rAd increased the stimulatory

capacity of human DC but without inducing polarization into Th1-driving APC. Production of the IL-12p40/35 heterodimer by DC is the key signal during the early steps of antigen presentation that drives differentiation of naive Th0 cells into Th1 lymphocytes (60). The fact that, in our system, rAd increased exclusively the transcription of IL-12p40 mRNA, without affecting basal levels of IL-12p35 transcripts, allows us to explain at a molecular level, the lack of Th1 polarization of rAd-infected DC reported previously (46).

Different pieces of evidence prompted us to investigate whether activation of the transcriptional factor NF- $\kappa$ B was involved in rAd-induced DC maturation: (i) components of hCMV, Epstein-Barr virus, herpes simplex virus, and human T-cell leukemia virus type 1 can activate NF- $\kappa$ B (2, 40); (ii) specific NF- $\kappa$ B DNA binding sequences ( $\kappa$ B motifs) are known to be present in the promoters of several of the genes that are upregulated by DC after rAd infection (2, 38, 51, 69, 70); and (iii) the NF- $\kappa$ B pathway is involved in the development and activation of myeloid DC (9, 10, 19, 43, 45, 48, 64). Our data indicate that there was rapid NF- $\kappa$ B activation in nuclei of DC within 1 h of rAd infection, probably as a consequence of virus-cell receptor interaction and/or internalization. The early NF- $\kappa$ B activation increased during the following 18 h. The late NF- $\kappa$ B activation suggests that viral gene transcription might have been responsible for NF- $\kappa$ B nuclear translocation, an unlikely mechanism based on the fact that both UV-irradiated and nonirradiated rAd exerted a similar effect on the BM DC. Another, more plausible explanation may be that, as a consequence of the early (within 1 h) NF- $\kappa$ B nuclear translocation, DC upregulated the transcription of certain proinflammatory cytokines (i.e., TNF- $\alpha$ ) that, in turn, may have induced a second phase of NF- $\kappa$ B activation (32).

There is evidence that rAd can activate NF- $\kappa$ B in other cell types, such as human vascular smooth muscle cells (11) and mouse hepatocytes (33). The mechanism(s) employed by rAd to activate NF- $\kappa$ B is unknown. In our experiments the effect did not depend on viral transcription. Consistent with these results, McCoy et al. (39) demonstrated that in vivo administration of UV-inactivated or incomplete Ad particles induced a strong inflammatory response in the respiratory tract. Borgland et al. reported recently that the chemokine induction occurring within 24 h of rAd infection in mice is mediated through capsid-dependent activation of NF- $\kappa$ B (7, 42). Taken together, these observations suggest that some of the viral components (DNA or proteins) are responsible for NF- $\kappa$ B activation.

In order for rAd to be adsorbed and then internalized by the host cell, the fiber knob must interact with the coxsackievirus and Ad receptor (CAR) and the penton base with  $\alpha_v\beta_3$  or  $\alpha_v\beta_5$  integrins (5, 62). The  $\alpha_M\beta_2$  integrin has been reported as the receptor for the penton protein of Ad2 in human hematopoietic cells (21). DC do not express CAR but do exhibit moderate levels of  $\alpha_v\beta_3$ ,  $\alpha_v\beta_5$ , and  $\alpha_M\beta_2$  integrins (46, 59). Both immature and mature DC are infectable by rAd in humans and mice (46, 59). It is likely that interaction between the Ad fiber and the integrins expressed on the DC surface may activate the NF- $\kappa$ B pathway (50, 68). It has been reported that the  $\alpha_v\beta_5$ -dependent cell migration in carcinoma cell lines and the  $\alpha_v\beta_3$ -induced survival in endothelial cells are phenomena mediated through activation of NF- $\kappa$ B (50, 68). Penton capsid binding to cell surface integrins induces an enzymatic cascade that phosphorylates the mitogen-activated protein kinase and the phosphoinositide-3-OH kinase (8, 31). Whether these kinases, when activated after rAd infection, are involved in the phosphorylation and subsequent degradation of I $\kappa$ B in DC is still unknown. Disruption of endosomes by internalized Ad parti-

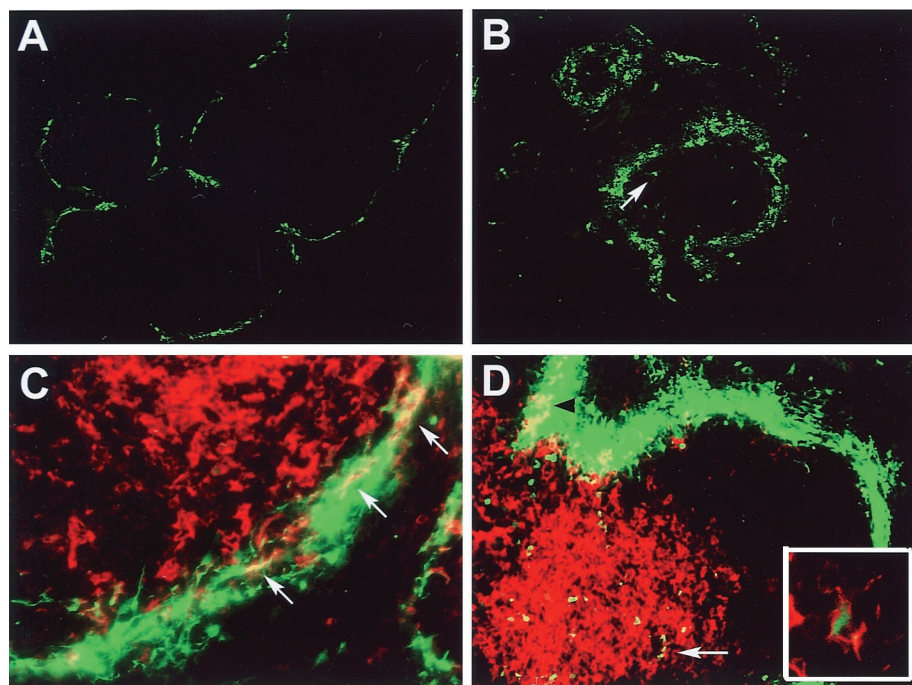


FIG. 8. Systemic administration of rAd-EGFP preferentially infects splenic DC in the marginal zone that later mobilize to the T-cell area. Mice were injected i.v. with rAd-EGFP and then killed at different time points. Sections of spleen were labeled with PE anti-CD11c MAb (C and D). Six hours after rAd administration, the expression of EGFP (in green) was confined exclusively to the marginal zones (A). At 24 h, the areas expressing the transgene became more diffuse, and EGFP<sup>+</sup> single cells with dendritic morphology were detected in the white pulp (B; arrow). (C) Detail of the marginal zone, 6 h after rAd-EGFP injection. DC coexpressing EGFP (in green) and CD11c (in red) are indicated in yellow (arrows). (D) 24 h following rAd-EGFP administration, DC coexpressing CD11c (in red) and EGFP (in green) are seen as yellow images in the marginal zone (black arrowhead at top left) and in the PALS (white arrow). (Inset) Detail of intracytoplasmic expression of EGFP (in green) in a CD11c<sup>+</sup> DC (in red) located in the PALS. Magnifications: A and B,  $\times 100$ ; C and D,  $\times 400$ ; Inset,  $\times 1,000$ . The composite illustrates representative images from three mice per time point, each analyzed for three different tissue sections.

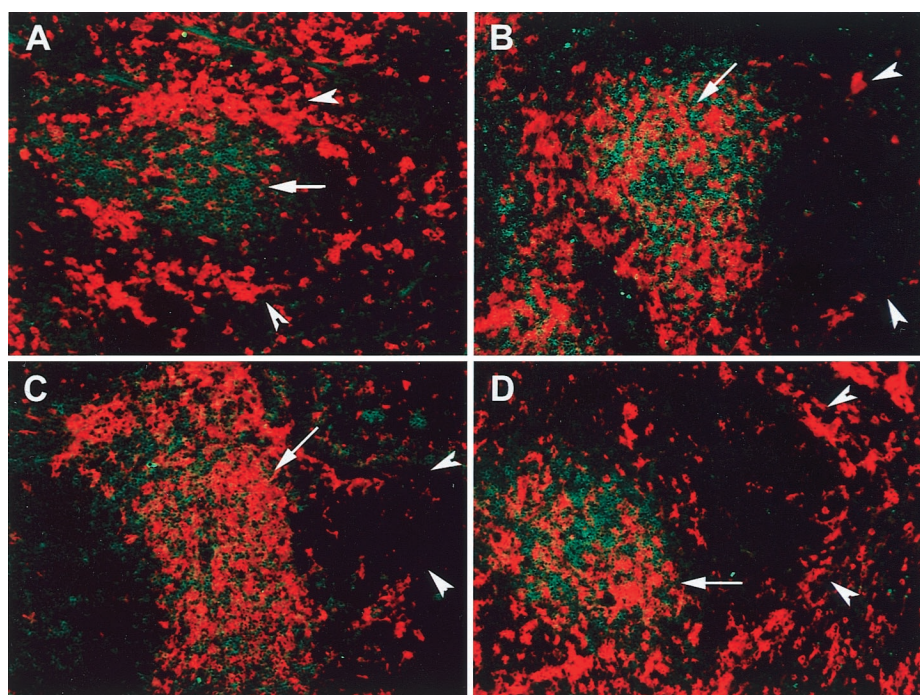


FIG. 9. Mobilization of DC from the marginal zone to the PALS following systemic administration of rAd. Mice were injected i.v. with rAd-Control and killed at different time points. Sections of spleen were double labeled with PE-anti-CD11 MAb and FITC-anti-CD3e MAb. Splenic DC are shown in red, and T cells are shown in green. DC located in the marginal zone are indicated by arrowheads, and DC in the PALS by arrows. (A) Under normal conditions, two subpopulations of CD11c<sup>+</sup> DC are clearly detected in the marginal zone and in the T-cell areas, respectively. The number of DC decreased in the marginal zone and increased in the T-cell area 6 and 24 h following systemic administration of rAd (B and C, respectively). (D) At 48 h after rAd administration, the marginal zone was repopulated with DC (arrowheads). Magnification,  $\times 200$ . The composite illustrates representative images from three mice per time point, each analyzed for three different tissue sections.

cles, with the subsequent release of proteolytic enzymes and viral DNA into the cytosol, has been also proposed as a possible mechanism of NF- $\kappa$ B activation (11). Unmethylated CpG bacterial DNA sequences have been demonstrated to activate NF- $\kappa$ B and trigger maturation of DC (54). However, in the present work, the induction of DC differentiation by CpG sequences present in transgenic DNA of rAd seems unlikely, since rAd encoding no transgene, or vectors encoding different transgenic cDNAs lacking CpG motifs, produced the same effect in DC.

We demonstrated that, within 6 h of systemic administration of rAd-EGFP, there was exclusive expression of the transgene in the splenic marginal zone, a region populated mainly by immature DC, B cells, and specialized macrophages (23, 56, 63). A considerable proportion of EGFP<sup>+</sup> cells in the marginal zone were also positive for the DC marker CD11c. Immature DC of the marginal zone are able to differentiate and migrate to the PALS after i.v. administration of LPS or soluble *T. gondii* antigen (14,47). Using a similar in vivo model, we demonstrated that, by 6 and 24 h after rAd i.v. injection, splenic DC rapidly mobilized to the T-cell-dependent areas, a phenomenon accompanied by a proportional decrease in the DC number in the marginal zone. Interestingly, not all mobilized DC expressed the transgene. This observation suggests that rAds might induce DC differentiation by different mechanisms: first, and as we demonstrated here in vitro, by direct stimulation of infected DC through NF- $\kappa$ B activation; and second, by induction of proinflammatory cytokines in DC or other neighboring cells that, in turn, trigger the maturation of nontransduced DC.

In conclusion, the data presented herein strongly suggest that rAd accelerates the differentiation of immature mouse DC, a phenomenon that is linked to activation of the transcription factor NF- $\kappa$ B. The enhancement of the stimulatory ability of DC induced by rAd may be the basis of the strong immune response elicited against rAd. It may explain the success of therapies based on rAd-transduced DC against neoplasms and infectious agents. However, the rAd effect on DC can be an obstacle when rAd-transduced DC are required to promote tolerance to treat autoimmune disease or to avoid graft rejection. The fast NF- $\kappa$ B activation induced by rAd in different cell types might explain the systemic inflammatory response and the activation of innate immunity reported recently as side effects of rAd in human clinical trials (36).

#### ACKNOWLEDGMENTS

We thank Nancy Zurowski and Bridget Colvin for skillful assistance with cell culture techniques, A. Shaked (Department of Surgery, University of Pennsylvania) for the rAd Add1434, D. A. Brenner (University of North Carolina) and A. Gambotto (University of Pittsburgh) for the rAd-I $\kappa$ B, and Cipriano Almonte and Simon Watkins for image processing. We thank Schering-Plough Research Institute, Kenilworth, N.J., for gifts of cytokines.

This study was supported by National Institutes of Health grants DK 49745 and AI 41011 (to A.W.T.) and by an NRSA grant (F32-GM-19877) from the National Institutes of Health (to R.W.G.).

#### REFERENCES

1. Arthur, J. F., L. H. Butterfield, M. D. Roth, L. A. Bui, S. M. Kiertscher, R. Lau, S. Dubinett, J. Glaspy, W. H. McBride, and J. Economou. 1997. A comparison of gene transfer methods in human dendritic cells. *Cancer Gene Ther.* **4**:17–25.
2. Baldwin, A. S., Jr. 1996. The NF- $\kappa$ B and I $\kappa$ B proteins: new discoveries and insights. *Annu. Rev. Immunol.* **14**:649–683.
3. Banchereau, J., and R. M. Steinman. 1998. Dendritic cells and the control of immunity. *Nature* **392**:245–322.
4. Bell, D., J. W. Young, and J. Banchereau. 1999. Dendritic cells. *Adv. Immunol.* **72**:255–322.
5. Bergelson, J. M., A. Krithivas, L. Celi, G. Droguett, M. S. Horwitz, T. Wickham, R. L. Crowell, and R. W. Finberg. 1998. The murine CAR homolog is a receptor for coxsackie B virus and adenoviruses. *J. Virol.* **72**:415–419.
6. Bhardwaj, N. 1997. Interactions of viruses with dendritic cells: a double-edged sword. *J. Exp. Med.* **186**:795–799.
7. Borgland, S. L., G. P. Bowen, Norman C. W. Wong, T. A. Libermann, and D. A. Muruve. 2000. Adenovirus vector-induced expression of the C-X-C chemokine IP-10 is mediated through capsid-dependent activation of NF- $\kappa$ B. *J. Virol.* **74**:3941–3947.
8. Bruder, G. T., and I. Kovesdi. 1997. Adenovirus infection stimulates the Raf/MAPK signaling pathway and induces interleukin-8 expression. *J. Virol.* **71**:398–404.
9. Burkly, L., C. Hession, L. Ogata, C. Reilly, L. A. Marconi, D. Olson, R. Tizard, R. Cate, and D. Lo. 1995. Expression of relB is required for the development of thymic medulla and dendritic cells. *Nature* **373**:531–536.
10. Carrasco, D., R. P. Ryseck, and R. Bravo. 1993. Expression of relB transcripts during lymphoid organ development: specific expression in dendritic antigen-presenting cells. *Development* **118**:1221–1231.
11. Clesham, G. J., P. J. Adam, D. Proudfoot, P. D. Flynn, S. Efstathiou, and P. L. Weissberg. 1998. High adenoviral loads stimulate NF $\kappa$ B-dependent gene expression in human vascular smooth muscle cells. *Gene Ther.* **5**:174–180.
12. Condon, C., S. C. Watkins, C. M. Celluzzi, K. Thompson, and L. D. Falo. 1996. DNA-based immunization by in-vivo transfection of dendritic cells. *Nat. Med.* **2**:1122–1128.
13. Cotten, M., M. Saltik, M. Kurs, E. Wagner, G. Maass, and M. L. Birnstiel. 1994. Psoralen treatment of adenovirus particles eliminates virus replication and transcription while maintaining the endosomolytic activity of the virus capsid. *Virology* **205**:254–261.
14. De Smedt, T., B. Pajak, E. Muraille, L. Lespagnard, E. Heinen, P. De Baetselier, J. Urbain, O. Leo, and M. Moser. 1996. Regulation of dendritic cell numbers and maturation by lipopolysaccharide in vivo. *J. Exp. Med.* **184**:1413–1424.
15. Di Nicola, M., S. Siena, M. Bregni, P. Longoni, M. Magni, M. Milanese, P. Mettaucci, R. Mortarini, A. Anichini, G. Parmiani, I. Drexler, V. Erffle, G. Sutter, and A. M. Gianni. 1998. Gene transfer into human dendritic antigen-presenting cells by vaccinia virus and adenovirus vectors. *Cancer Gene Ther.* **5**:350–356.
16. Dietz, A. B., and S. Vuk-Pavlovic. 1998. High efficiency adenovirus-mediated gene transfer to human dendritic cells. *Blood* **91**:392–398.
17. Flomenberg, P., V. Piskowski, R. L. Truitt, and J. T. Casper. 1995. Characterization of human proliferative responses to adenovirus. *J. Infect. Dis.* **171**:1090–1096.
18. Graham, F. L., and L. Prevec. 1995. Methods for construction of adenovirus vectors. *Mol. Biotech.* **3**:207–220.
19. Graneli-Piperno, A., M. Pope, K. Inaba, and R. M. Steinman. 1995. Coexpression of NF $\kappa$ B/Rel and Sp1 transcription factors in human immunodeficiency virus 1-induced, dendritic cell-T-cell syncytia. *Proc. Natl. Acad. Sci. USA* **92**:10944–10948.
20. Henkel T., T. Machleidt, I. Alkalay, M. Kronke, Y. Ben-Nerlah, and P. A. Baeuerle. 1993. Rapid proteolysis of I $\kappa$ B- $\alpha$  is necessary for activation of transcription factor NF- $\kappa$ B. *Nature* **365**:182–185.
21. Huang, S., T. Kamata, Y. Takada, Z. M. Ruggeri, and G. R. Nemerow. 1996. Adenovirus interaction with distinct integrins mediates separate events in cell entry and gene delivery to hematopoietic cells. *J. Virol.* **70**:4502–4508.
22. Inaba, K., M. Inaba, N. Romani, H. Aya, M. Deguchi, S. Ikehara, S. Muramatsu, and R. M. Steinman. 1992. Generation of large numbers of dendritic cells from mouse bone marrow cultures supplemented with granulocyte/macrophage colony-stimulating factor. *J. Exp. Med.* **176**:1693–1702.
23. Inaba, K., M. Witmer-Pack, M. Inaba, K. S. Hathcock, H. Sakuta, M. Azuma, H. Yagita, K. Okumura, P. S. Linsley, S. Ikehara, S. Muramatsu, R. J. Hodes, and R. M. Steinman. 1994. The tissue distribution of the B7-2 costimulator in mice: abundant expression on dendritic cells in situ and during maturation in vitro. *J. Exp. Med.* **180**:1849–1860.
24. Jobin, C., A. Panja, C. Hellerbrand, Y. Iimuro, J. Didonato, D. A. Brenner, and R. B. Sartor. 1998. Inhibition of proinflammatory molecule production by adenovirus-mediated expression of a nuclear factor  $\kappa$ B super-repressor in human intestinal epithelial cells. *J. Immunol.* **160**:410–418.
25. Jonuleit, H., T. Tuting, J. Steitz, J. Bruck, A. Giesecke, K. Steinbrink, J. Knop, and A. H. Enk. 2000. Efficient transduction of mature CD83<sup>+</sup> dendritic cells using recombinant adenovirus suppressed T cell stimulatory capacity. *Gene Ther.* **7**:249–254.
26. Kafri, T., D. Morgan, T. Kralh, N. Sarvetnick, L. Sherman, and I. Verma. 1998. Cellular immune response to adenoviral vector infected cells does not require de novo viral gene expression: implications for gene therapy. *Proc. Natl. Acad. Sci. USA* **95**:11377–11382.
27. Kaplan, J. M., Q. Yu, S. T. Piraino, S. E. Pennington, S. Shankara, L. A. Woodworth, and B. L. Roberts. 1999. Induction of antitumor immunity with dendritic cells transduced with adenovirus vector-encoding endogenous tumor-associated antigens. *J. Immunol.* **163**:699–707.
28. Karin, M., and M. Delhase. 2000. The I kappa B kinase (IKK) and NF-kappa B: key elements of proinflammatory signaling. *Semin. Immunol.* **12**:85–98.
29. Kirk, C. J., and J. J. Mule. 2000. Gene-modified dendritic cells for use in

- tumor vaccines. *Hum. Gene Ther.* **11**:797–806.
30. Lee, W.-C., C. Zhong, S. Qian, Y. Wan, J. Gaudie, Z. Mi, P. D. Robbins, A. W. Thomson, and L. Lu. 1998. Phenotype, function, and in vivo migration and survival of allogeneic dendritic cell progenitors genetically engineered to express TGF $\beta$ . *Transplantation* **66**:1810–1817.
  31. Li, E., D. Stupack, R. Klemke, D. A. Cheresch, and G. R. Nemerow. 1998. Adenovirus endocytosis via  $\alpha$ (v) integrins requires phosphoinositide-3-OH kinase. *J. Virol.* **72**:2055–2061.
  32. Lieber, A., C. Y. He, L. Meuse, C. Himeda, C. Wilson, and M. A. Kay. 1998. Inhibition of NF- $\kappa$ B activation in combination with bcl-2 expression allows for persistence of first-generation adenovirus vectors in the mouse liver. *J. Virol.* **72**:9267–9277.
  33. Lieber, A., C. Y. He, L. Meuse, D. Schowalter, I. Kirillova, B. Winther, and M. A. Kay. 1997. The role of Kupffer cell activation and viral gene expression in early liver toxicity after infusion of recombinant adenovirus vectors. *J. Virol.* **71**:8798–8807.
  34. Lotze, M. T., and A. W. Thomson (ed.). 1999. *Dendritic cells: biology and clinical applications*. Academic Press, San Diego, Calif.
  35. Lu, L., A. Gambotto, W.-C. Lee, S. Qian, C. A. Bonham, P. D. Robbins, and A. W. Thomson. 1999. Adenoviral delivery of CTLA4Ig into myeloid dendritic cells promotes their in vitro tolerogenicity and survival in allogeneic recipients. *Gene Ther.* **6**:554–563.
  36. Marshall, E. 1999. Gene therapy death prompts review of adenovirus vector. *Science* **286**:2244–2245.
  37. Masurier, C., C. Pioche-Durieu, B. M. Colombo, R. Lacave, F. M. Lemoine, D. Klatzmann, and M. Guigon. 1999. Immunophenotypical and functional heterogeneity of dendritic cells generated from murine bone marrow with different cytokine combinations: implications for anti-tumoral cell therapy. *Immunology* **96**:569–577.
  38. May, M. J., and S. Ghosh. 1998. Signal transduction through NF- $\kappa$ B. *Immunol. Today* **19**:80–88.
  39. McCoy, R. D., B. L. Davidson, B. J. Roessler, G. B. Huffnagle, S. L. Janich, T. J. Laing, and R. H. Simon. 1995. Pulmonary inflammation induced by incomplete or inactivated adenoviral particles. *Hum. Gene Ther.* **6**:1553–1560.
  40. Mosialos, G. 1997. The role of Rel/NF- $\kappa$ B proteins in viral oncogenesis and the regulation of viral transcription. *Semin. Cancer Biol.* **8**:121–129.
  41. Mulders, P., S. Pang, J. Dannull, R. Kaboo, A. Hinkel, K. Michel, C. L. Tso, M. Roth, and A. Beldegrun. 1998. Highly efficient and consistent gene transfer into dendritic cells utilizing a combination of ultraviolet-irradiated adenovirus and poly(L-lysine) conjugates. *Cancer Res.* **58**:956–961.
  42. Muruve, D. A., M. J. Barnes, I. E. Stillman, and T. A. Libermann. 1999. Rapid induction of multiple chemokines by replication-deficient adenoviral vectors results in acute neutrophil-dependent hepatic toxicity in vivo. *Hum. Gene Ther.* **10**:965–976.
  43. Neumann, M., H.-W. Fries, C. Scheicher, P. Keikavoussi, A. Kolb-Maurer, E.-B. Brocker, E. Serfling, and E. Kampgen. 2000. Differential expression of Rel/NF- $\kappa$ B and octamer factors is a hallmark of the generation and maturation of dendritic cells. *Blood* **95**:277–285.
  44. Olthoff, K. M., T. A. Judge, A. E. Gelman, X. da Shen, W. W. Hancock, L. A. Turka, and A. Shaked. 1998. Adenovirus-mediated gene transfer into cold-preserved liver allografts: Survival pattern and unresponsiveness following transduction with CTLA4Ig. *Nat. Med.* **4**:194–200.
  45. Pettit, A. R., C. Quinn, K. P. MacDonald, L. L. Cavanagh, G. Thomas, W. Townsend, M. Handel, and R. Thomas. 1997. Nuclear localization of RelB is associated with effective antigen-presenting cell function. *J. Immunol.* **159**:3681–3691.
  46. Rea, D., F. H. Schagen, R. C. Hoeben, M. Mehtali, M. J. E. Havenga, R. E. M. Toes, C. J. M. Melief, and R. Offringa. 1999. Adenovirus activate human dendritic cells without polarization toward a T-helper type 1-inducing subset. *J. Virol.* **73**:10245–10253.
  47. Reis e Sousa, C., S. Hieny, T. Scharton-Kersten, D. Jankovic, H. Charest, R. N. Germain, and A. Sher. 1997. In vivo microbial stimulation induces rapid CD40 ligand-independent production of interleukin 12 by dendritic cells and their distribution to T cell areas. *J. Exp. Med.* **186**:1819–1829.
  48. Rescigno, M., M. Martino, C. L. Sutherland, M. R. Gold, and P. Ricciardi-Castagnoli. 1998. Dendritic cell survival and maturation are regulated by different signaling pathways. *J. Exp. Med.* **188**:2175–2180.
  49. Romani, N., M. Witmer-Pack, M. Crowley, S. Koide, G. Schuler, K. Inaba, and R. Steinman. 1991. Langerhans cells as immature dendritic cells, p. 191–216. *In* G. Schuler (ed.), *Epidermal Langerhans cells*. CRC Press, Inc., Boca Raton, Fla.
  50. Scatena, M., M. Almeida, M. L. Chaisson, N. Fausto, R. F. Nicosia, and C. M. Giachelli. 1998. NF- $\kappa$ B mediates  $\alpha$ 5 $\beta$ 3 integrin-induced endothelial cell survival. *J. Cell Biol.* **141**:1083–1093.
  51. Sica, A., L. Dorman, V. Viggiano, M. Cippitelli, P. Ghosh, N. Rice, and H. A. Young. 1997. Interaction of NF- $\kappa$ B and NFAT with the interferon- $\gamma$  promoter. *J. Biol. Chem.* **272**:30412–30420.
  52. Smith, C. A., L. S. Woodruff, G. R. Kitchingman, and C. M. Rooney. 1996. Adenovirus-pulsed dendritic cells stimulate human virus-specific T-cell responses in vitro. *J. Virol.* **70**:6733–6740.
  53. Souberbielle, B. E., and W. C. Russell. 1995. Human T cell proliferative response to polypeptides from adenovirus type 2. *J. Infect. Dis.* **172**:1421–1422.
  54. Sparwasser, T., E.-S. Koch, R. M. Vabulas, K. Heeg, G. B. Lipford, J. W. Ellwart, and H. Wagner. 1998. Bacterial DNA and immunostimulatory CpG oligonucleotides trigger maturation and activation of murine dendritic cells. *Eur. J. Immunol.* **28**:2045–2054.
  55. Steptoe, R. J., and A. W. Thomson. 1996. Dendritic cells and tolerance induction. *Clin. Exp. Immunol.* **105**:397–402.
  56. Steinman, R. M., M. Pack, and K. Inaba. 1997. Dendritic cells in the T-cell areas of lymphoid organs. *Immunol. Rev.* **156**:25–37.
  57. Takayama, T., Y. Nishioka, L. Lu, M. T. Lotze, H. Tahara, and A. W. Thomson. 1998. Retroviral delivery of viral IL-10 into myeloid dendritic cells markedly inhibits their allostimulatory activity and promotes the induction of T cell hyporesponsiveness. *Transplantation* **66**:1567–1574.
  58. Thomson, A. W., and L. Lu. 1999. Are dendritic cells the key to liver transplant tolerance? *Immunol. Today* **20**:27–32.
  59. Tillman, B. W., T. D. de Grujil, S. A. Luyck-de Bakker, R. J. Scheper, H. M. Pinedo, T. J. Curiel, W. R. Gerritsen, and D. T. Curiel. 1999. Maturation of dendritic cells accompanies high-efficiency gene transfer by CD40-targeted adenoviral vector. *J. Immunol.* **162**:6378–6383.
  60. Trinchieri, G. 1998. Interleukin-12: a cytokine at the interface of inflammation and immunity. *Adv. Immunol.* **70**:83–243.
  61. Van Tendeloo, V. F. I., H.-W. Snoeck, F. Lardon, G. L. E. E. Vanham, G. Nijs, M. Lenjou, L. Hendricks, C. van Broeckhoven, A. Mouljijn, I. Rodrigus, P. Verdonk, D. R. Van Bockstaele, and Z. N. Berneman. 1998. Nonviral transfection of distinct types of human dendritic cells: high efficiency gene transfer by electroporation into hematopoietic progenitor but not monocyte-derived dendritic cells. *Gene Ther.* **5**:700–707.
  62. Wickham, T. J., P. Mathias, D. A. Cheresch, and G. R. Nemerow. 1993. Integrins  $\alpha$ V $\beta$ 3 and  $\alpha$ V $\beta$ 5 promote adenovirus internalization but not virus attachment. *Cell* **73**:309–319.
  63. Witmer, M. D., and R. M. Steinman. 1984. The anatomy of peripheral lymphoid organs with emphasis on accessory cells: light-microscopy immunocytochemical studies of mouse spleen, lymph node, and Peyer's patch. *Am. J. Anat.* **170**:465–481.
  64. Wu, L., A. D'Amico, K. D. Winkel, M. Suter, D. Lo, and K. Shortman. 1998. RelB is essential for the development of myeloid-related CD8 $\alpha^+$  dendritic cells but not of lymphoid-related CD8 $\alpha^+$  dendritic cells. *Immunity* **9**:839–847.
  65. Yang, Y., F. A. Nunes, K. Berencsi, E. E. Furth, E. Gonczol, and J. M. Wilson. 1994. Cellular immunity to viral antigens limits E1-deleted adenovirus for gene therapy. *Proc. Natl. Acad. Sci. USA* **91**:4407–4411.
  66. Yang, Y., H. C. J. Ertl, and J. M. Wilson. 1994. MHC class I restricted cytotoxic T lymphocytes to viral antigens destroy hepatocytes in mice infected with E1 deleted recombinant adenovirus. *Immunity* **1**:433–442.
  67. Yang, Y., Q. Li, H. C. J. Ertl, and J. M. Wilson. 1995. Cellular and humoral immune responses to viral antigens create barriers to lung-directed gene therapy with recombinant adenoviruses. *J. Virol.* **69**:2004–2015.
  68. Yebra, M., E. J. Filardo, E. M. Bayna, E. Kawahara, J. C. Becker, and D. A. Cheresch. 1995. Induction of carcinoma cell migration on vitronectin by NF- $\kappa$ B-dependent gene expression. *Mol. Biol. Cell* **6**:841–850.
  69. Yoshimoto, T., H. Nagase, T. Ishida, J. Inoue, and H. Nariuchi. 1997. Induction of interleukin-12 p40 transcript by CD40 ligation via activation of nuclear factor- $\kappa$ B. *Eur. J. Immunol.* **27**:3461–3470.
  70. Zhao, J., G. J. Freeman, G. S. Gray, L. M. Nadler, and L. H. Glimcher. 1996. A cell type-specific enhancer in the human B7.1 gene regulated by NF- $\kappa$ B. *J. Exp. Med.* **183**:777–789.
  71. Zhong, L., A. Granelli-Piperno, Y. Choi, and R. M. Steinman. 1999. Recombinant adenovirus is an efficient and non-perturbing genetic vector for human dendritic cells. *Eur. J. Immunol.* **29**:964–972.